



ISME

One Dimensional Internal Ballistics Simulation of Solid Rocket Motor

S. Gh. Moshir Stekhareh^{*}
Researcher

A. R. Mostofizadeh[†]
Assistant Professor

N. Fouladi[‡]
Associated Professor

A. Soleymani[§]
PHD Student

An internal ballistics model has been developed for performance prediction of a solid propellant rocket motor. In this model a 1-D unsteady Euler equation with source terms is considered. The flow is assumed as a non-reacting mixture of perfect gases with space and time varying thermo physical properties. The governing equations in the combustion chamber are solved numerically by using the Steger and Warming flux vector splitting scheme. After validation of results by experimental data, the effect of grain geometrical variables and solid propellant characteristics are studied on performance characteristics of a standard internal burning cylindrical grain. These parameters include of negative /positive erosive burning, propellant characteristics, port to throat area ratio and initial temperature of the propellant. The results of developed model show that, propellant characteristics are dominant factors which affect performance characteristics. When erosive burning rate are considered, the 1-D internal ballistic analysis have good agreement with experimental data.

Keywords: Ballistic, Solid Rocket motor, Unsteady, Euler, Grain

1 Introduction

The internal ballistics analysis of solid propellant rocket motors (SRM's) describe the internal flow through the core (port) of grain where the input mass is added from the burning surface of the solid propellant. In design and development procedure of SRM's, the improvement of internal ballistics prediction capabilities will lead to improvement of SRM's reliability and reduction in the design and development costs, which are related to experimental activities and static firing tests.

^{*} Corresponding Author, Researcher, Department of Mechanical and Aerospace Engineering, Malek e Ashtar University of Technology, ghasemmoshir@yahoo.com

[†] Assistant Professor, Department of Mechanical and Aerospace Engineering, Malek e Ashtar University of Technology, armostofizadeh@mut-es.ac.ir

[‡] Associated Professor, Department of Mechanical and Aerospace Engineering, Malek e Ashtar University of Technology, N_Fouladi@yahoo.com

[§] PHD Student, Department of Mechanical and Aerospace Engineering, Malek e Ashtar University of Technology, ardalan_soleymani@yahoo.com

Detail representation of main physical phenomena in combustion chamber of SRM's and also acceptable computational time are two important advantages of using one dimensional unsteady flow filed model in internal ballistics simulations.

Greatrix had worked on the effect of acceleration field on burning rate [1]. Attili solved the quasi steady state for internal ballistics simulations [2]. In the Wilcox paper two different burning rate models was investigated [3]. Cavalini studied the effect of erosive burning rate on head end pressure [4]. Terzic used a modular computer program named SPPMEF which is intended for purposes of predicting internal ballistic performances of solid propellant rocket motors [5].

In the past papers, the 1-D unsteady Euler equation was solved by finite volume method and effect of some parameters on head end pressure was investigated [1-5]. In this paper with special attention to computation time, by using finite difference method, 1-D unsteady Euler equation is solved. The effect of erosive burning, propellant characteristics and the port to throat area ratio on head end pressure of a SRM with cylindrical grain are studied. In addition analytical burn back of grain and also flow field parameters such as velocity, pressure and temperature in combustion chamber are investigated.

2 Internal ballistics of the SRM's

By using differential form of conservation laws for mass, momentum and energy with the perfect gas equation of state, the internal ballistics of the SRMs could be simulated [6]. The unsteady 1-D form of conservation laws for an axial gas flow, in flux vector presentation could be expressed as:

$$\frac{\partial Q}{\partial t} + \frac{\partial E}{\partial x} = H \quad (1)$$

Where

$$Q = \begin{bmatrix} \rho \\ \rho u \\ \rho e_t \end{bmatrix} \text{ and } E = \begin{bmatrix} \rho u \\ \rho u^2 + p \\ (\rho e_t + p)u \end{bmatrix} \quad (2)$$

And also

$$H = \begin{bmatrix} -\frac{1}{A_p} \frac{\partial A_p}{\partial x} \rho u - \left(\frac{1}{A_p} \frac{\partial A_p}{\partial t} + r_b \frac{P_b}{A_p} \right) \rho + \rho_s r_b \frac{P_b}{A_p} \\ -\frac{1}{A_p} \frac{\partial A_p}{\partial x} \rho u^2 - \left(\frac{1}{A_p} \frac{\partial A_p}{\partial t} + r_b \frac{P_b}{A_p} \right) \rho u \\ -\frac{1}{A_p} \frac{\partial A_p}{\partial x} (\rho u e_t + up) - \left(\frac{1}{A_p} \frac{\partial A_p}{\partial t} + r_b \frac{P_b}{A_p} \right) \rho e_t + \rho_s r_b \frac{P_b}{A_p} \left(C_p T_f + \frac{(\rho_s r_b / \rho)^2}{2} \right) \end{bmatrix} \quad (3)$$

In equation (1), A_p is grain port cross section area that varies over time and along port axis, and also $e_t = \frac{p}{(\gamma-1)\rho} + \frac{u^2}{2}$. In order to solve equation (1), a finite difference scheme based on Steger and Warming flux vector splitting was used that is an implicit method [7].

Simultaneously Solving equation (1), leads to determination of pressure, velocity, temperature, and other internal flow parameters along the axis port of the grain. As shown in equation (4) mass addition rate is calculated by the product of the burning rate (from burning rate model, r_b), burning surface (from grain geometry prediction model, S_b) and the solid propellant density.

$$\dot{m}_{add} = \rho_s S_b r_b \quad (4)$$

Because of numerical stability considerations, the time step was set to 1.e-6 and Courant–Friedrichs–Lewy Number (CFL Number) was limited to 0.2. The number of grids inside the motor was 708 and inside the convergence part of nozzle was 20. By using this generated mesh, the CPU time was 1400 sec. The processor was Pentium® Dual-Core CPU T4500 @ 2.30 GHz and effective memory was 3.00 GB.

2-1- Boundary condition

Two boundary conditions were introduced, at the head end of the motor, velocity is set to zero and at the other end, in nozzle throat, by mean of characteristic method, can be determined. If flow in throat is supersonic, then all the characteristics leave the domain and, as a result, boundary condition can be specified by extrapolation scheme, Otherwise If flow is subsonic, an analytical boundary condition may be specified; and other two are determined from the interior solution by extrapolation [6]. Analytical boundary condition could be specified by equation (5):

$$p = p_1 \left(1 - \frac{u^2 - u_1^2}{\frac{2\gamma}{\gamma-1} RT_1} \right)^{\frac{\gamma}{\gamma-1}} \quad (5)$$

In equation (5), p_1 , u_1 and T_1 are thermodynamic properties of combustion products at the entrance of nozzle.

2-2 Burning Rate Model

The combustion mechanisms of solid propellants are quite complex and depend on many local chemical, thermal and fluid flow phenomena. Many solid propellant burning-rate models are greatly simplified because of limited computational power and understanding of the combustion process. In this study, The Saint Robert's law was used which approximates the burning rate as solely dependent on the mean local pressure [8]. Equation (6) shows the Saint Robert's law:

$$r_0 = ap^n \quad (6)$$

Where r_0 is burning rate, a and n are propellant-dependent empirically measured constants. a is known as the temperature coefficient and n is known as the burning rate exponent, it sometimes called the combustion index. In order to increase internal ballistics simulation accuracy, the effects of erosive burning phenomenon can be added to model. Erosive burning becomes important in SRMs with high port axial velocity which leads to increasing heat transfer to the solid propellant that leads to increasing the local burning rate. This typically occurs in motors with large aspect ratios (L/D , L is the motor length and D is the grain diameter). A relatively simple model for erosive burning, based on heat transfer, was first developed in 1956 by Lenoir and Robillard and has been improved and used widely in motor performance calculations [9]. It is based on adding together two burn rates, r_0 , which primarily is a function of pressure and ambient grain temperature (equation (6)) without erosion effects, and r_e is the burning rate due to gas velocity or erosion effects:

$$r_b = r_0 + r_e = ap^n + \alpha G^{0.8} D^{-0.2} \exp(-\beta r \rho_s / G) \quad (7)$$

Which G is the mass flux ($\text{kg/m}^2\text{s}$), D is a characteristic dimension of the port passage (usually, $D = 4A_p / P_b$, where A_p is the port area and P_b is its perimeter) and α and β are empirically constants. Apparently, β is independent of propellant formulation and has a value of about 53 when r is in m/s . From heat transfer considerations α can be determined as:

$$\alpha = \frac{0.0288 C_p \mu^{0.2} \text{Pr}^{-2/3} T_f - T_s}{\rho_s C_s T_s - T_p} \quad (8)$$

In equation (8), Pr (prandtl number) is based on the combustion products properties.

3 Internal Ballistic Code Verification and Results

Numerical Results are presented for a SRM with standard internal burning cylindrical grain. Essential motor characteristics are summarized in Table (1):

Table 1 Motor and propellant characteristics

| | |
|------------------------------------------------------------------------|-----------------------------------------------------------|
| Propellant grain length(L) | 70.8 cm |
| Initial port diameter(d_i) | 2.54 cm |
| Inner casing diameter(d_f) | 6.35 cm |
| nozzle throat diameter(d_t) | 2.35 cm |
| Pressure dependent burning rate(r_0) | $4.92 \times 10^{-2} [p(\text{kpa})]^{0.36} \text{ cm/s}$ |
| Propellant specific heat(C_s) | 1508 j/kg.k |
| gas flame temperature(T_f) | 3056 k |
| solid propellant surface temperature(T_s) | 1128 k |
| initial ambient temperature within the solid propellant grain(T_p) | 294 k |
| propellant density(ρ_s) | 1742 kg/m^3 |
| Gas specific heat(C_p) | 1845 j/kg.k |
| Gas prandtl number(Pr) | 0.82 |
| Specific gas constant (R) | 318 j/kg.k |
| combustion products thermal conductivity(k) | 0.184 w/m.k |
| combustion products viscosity(μ) | $8.19 \times 10^{-5} \text{ kg/m.k}$ |
| Gas specific heat ratio(γ) | 1.21 |

Figure (1) represents the head end pressure for both experimental test and numerical prediction. As shown in figure (1), the experimental and simulated pressures have good agreement except at the beginning of combustion when the igniter ignites the solid propellant, the process of ignition is not simulated in this work, and because of that at the period of ignition the simulated pressure traces have been shifted. One of the most important goals in internal ballistic analysis is, finding the maximum pressure during the SRM operation. As shown in figure (1), there is good agreement between maximum predicted and measured pressure. Because of importance of erosive burning in typical SRMs, the head end pressure with and without erosive burning was considered and shown in figure (2).

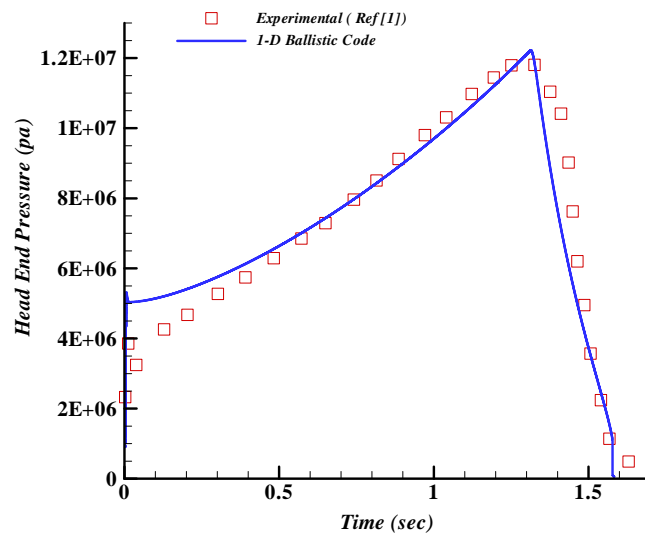


Figure 1 Experimental and simulated (1-D) head end pressure

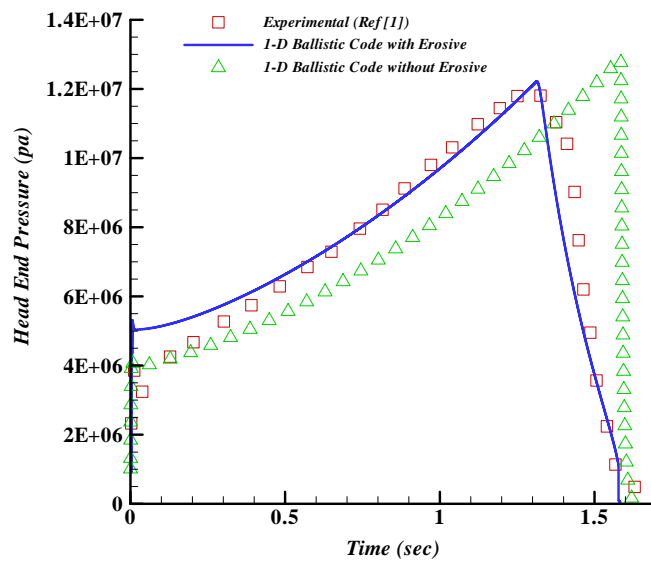


Figure 2 Comparison Erosive and Non-Erosive Burning Rate Consideration on Head End Pressure

The results show that consideration of erosive burning causes better agreement between predicted and measured head end pressure.

Figure (3) represents the effect of erosive and non-erosive burning rate and zero dimensional internal ballistic consideration on head end pressure. As seen in this figure, erosive burning consideration is a dominant physical phenomenon in SRMs performance predictions and

without considering that, Changes in flow parameters along the motor axis are negligible, hence the results for 1-D and 0-D internal ballistics analysis, is rather than same.

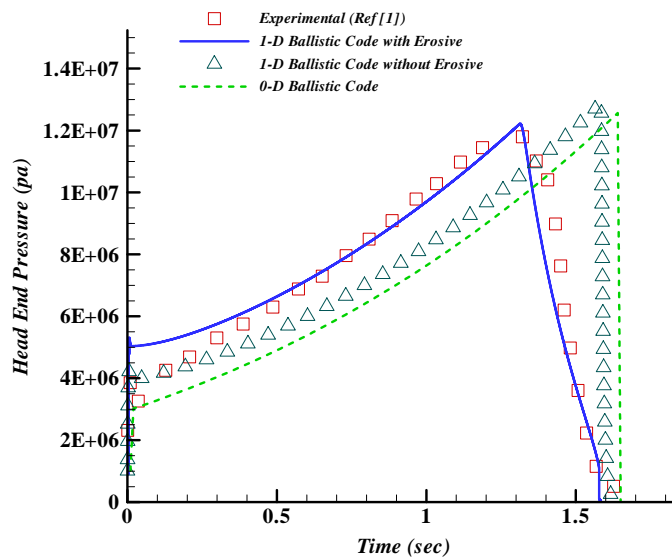


Figure 3 Comparison 1-D and 0-D internal ballistic Consideration on Head End Pressure

The effects of different type of propellant in terms of different temperature coefficient on head end pressure are shown figure (4).

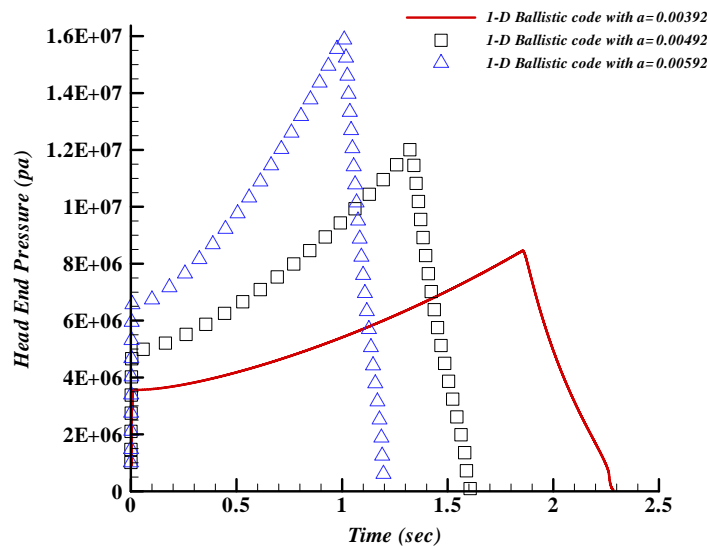


Figure 4 The Effect of Temperature Coefficient on Head End Pressure

The chamber pressure is affected by burning rate, on the other hand and According to equation (6), burning rate is varied due to changes in propellant temperature coefficient, so as the figure (4) Shows, It can be concluded that, the head end pressure is affected strongly by propellant characteristic especially, by the propellant temperature coefficient.

By considering erosive burning, the effect of variation in port to throat ratio on head end pressure could be expressed.

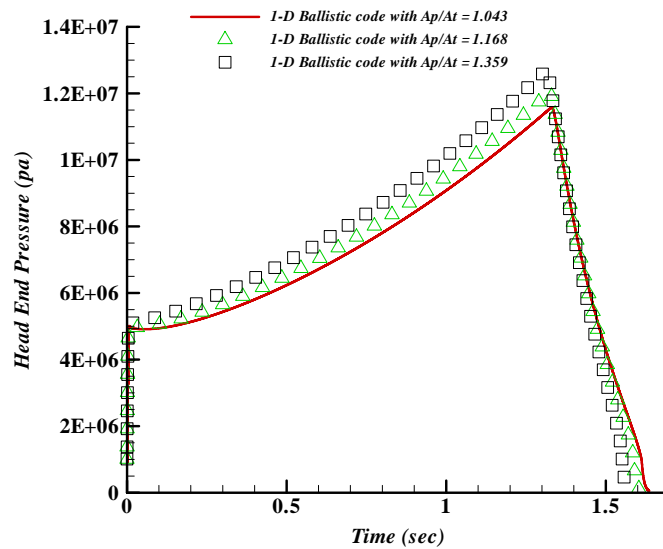


Figure 5 The Effect of Variation in Port to Throat Area Ratio on Head End Pressure

As shown in figure (5), when erosive burning is considered, upper value of port to throat area ratio leads to increasing the head end pressure.

To evaluate the effect of initial temperature of propellant on head end pressure, three values for initial temperatures were considered (244K, 294K and 344K). The sensitivity of burning rate to propellant temperature not considered.

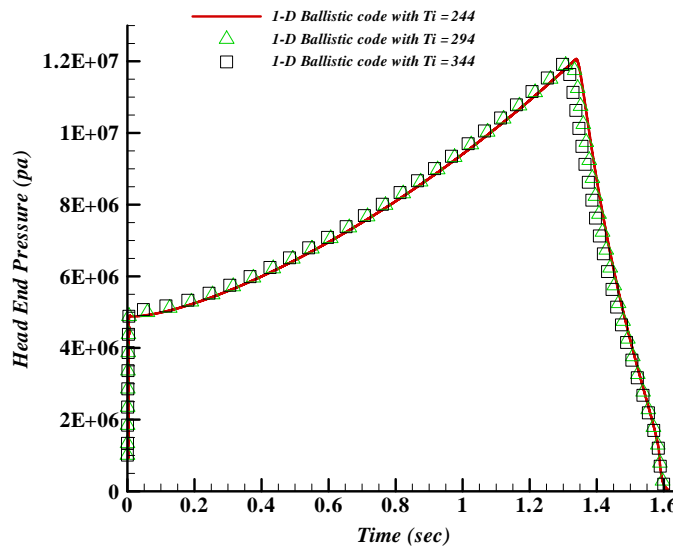


Figure 6 The Effect of Initial Temperature of the Propellant on Head End Pressure

According to figure (6) it can be concluded that variation in initial temperature of propellant negligibly affects the erosive burning rate. So by increasing by the initial temperature of the propellant, the head end pressure negligibly increased.

Local velocity and pressure variations along the port axis are shown in figure (7) and figure (8). As seen in the figure (7) and figure (8), during burning time, local axial port velocity along the port axis is decreased and simultaneously the local port pressure is increased.

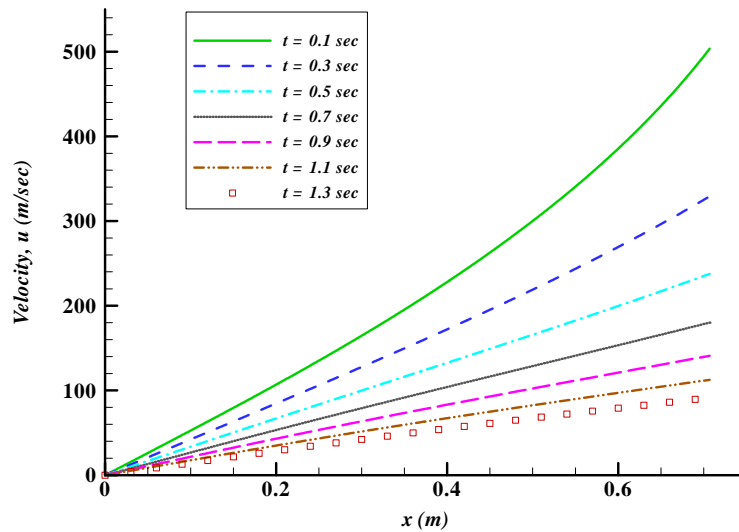


Figure 7 Variation of Local Port Velocity Along Port Axis During Burning Time

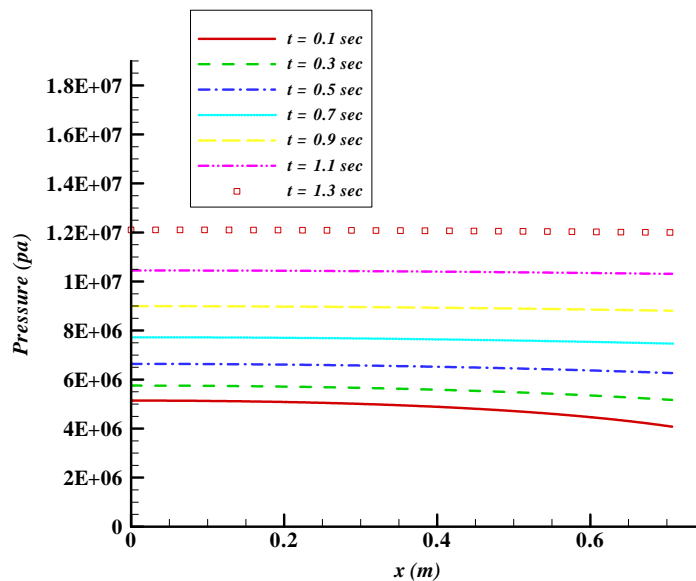


Figure 8 Variation of Local Port Pressure Along Port Axis During Burning Time

During burning time, the local pressure along port axis is increased, but pressure variation is not severe so it's acceptable to assume that pressure along the port axis is constant. Local temperature variation along port axis during burning time is shown in figure (9).

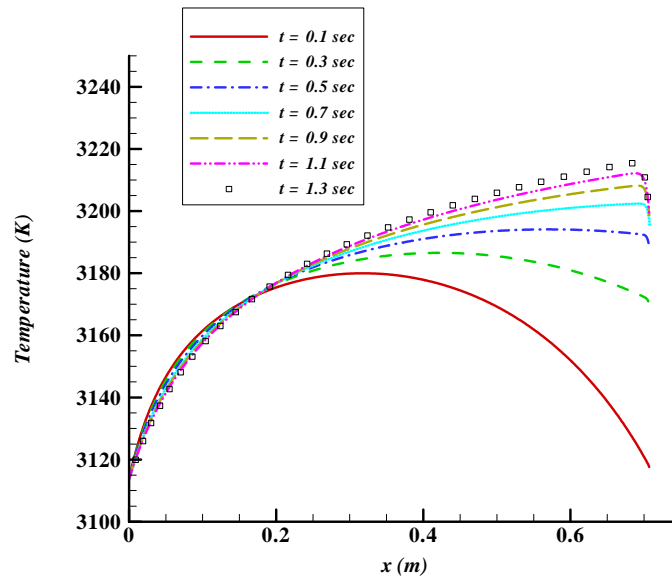


Figure 9 Variation of Local Port Temperature Along Port Axis During Burning Time

The results show that as the time passed, combustion products local temperature is increased. But this increment is up to 3%. So it's acceptable to say temperature along the port axis is constant. Variation of local port cross section area along port axis during burning time is shown in figure (10).

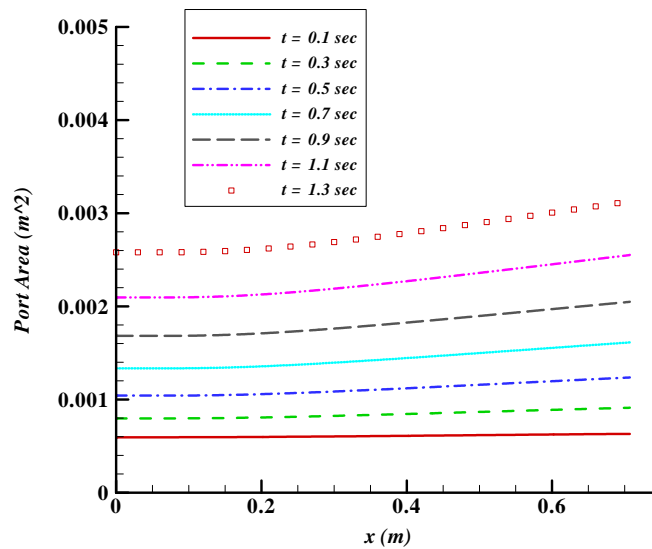


Figure 10 Variation of Local Port Cross Section Area Along Port Axis During Burning Time

The grain geometry which is used in this analysis is standard cylindrical internal burning. During burning time as the burning surface is burned back, port cross section area is increased. As seen in figure (10), variation of port area along the motor axis at the beginning of motor operation is negligible and port area can be assumed constant but as the time passed, because of erosive burning these variations are increased.

4 Conclusion

The numerical model has been presented for simulation of SRM unsteady internal flow and combustion which is fairly comprehensive. In order to reduce the computational time, the 1-D Euler equations were used. Using developed numerical model leads to low computational time and numerical results shown there is a good agreements between simulated and measured data. Erosive burning phenomenon has been modeled and comparison of simulated and measured data showed qualitative agreement has been obtained. It has seen that by increasing of port to throat area ratio, head end pressure was increased and temperature coefficient of burning rate affected the predicted head end pressure severely. Also it has seen that, when the sensitivity of burning rate to propellant temperature not consider, initial temperature of grain is not a dominant factor in performance simulation of SRMs. Local Pressure variations along the port were simulated and have seen that the variations are quiet negligible, so the pressure along port axis could be assumed constant.

The present simulation does not contain the effects of transient propellant burning. In SRM's transient burning effects often coupled the flow disturbances with combustion instabilities, so the results of this study should be considered as variation ballistic parameters and head end pressure.

References

- [1] Gottlieb, J. J., and Greatrix, D. R., "Numerical Study of the Effects of Longitudinal Acceleration on Solid Rocket Motor Internal Ballistics", *Fluids Engineering*, Vol. 114, pp. 404-411, (1992).
- [2] Attili, A., Favini, B., Di Giacinto, M., and Serraglia, F., "Numerical Simulation of Multi-phase Flow in Solid Rocket Motors", 6th European Symposium on Aerothermodynamics for Space Vehicles, France, (2008).
- [3] Willcox, M. A., Brewster, C. Q., Tang, K. M., and Stewart, S. D., "Solid Propellant Grain Design and Burnback Simulation using a Minimum Distance Function", *Propulsion and Power*, Vol. 23, No. 11, pp. 465-475, (2007).
- [4] Cavallini, E., Favini, B., and Di Giacinto, M., "Internal Ballistics Simulation of a NAWC Tactical SRM", *J. Applied Mechanics*, Vol. 78, pp. 510-518, (2011).
- [5] Terzic, J., Zecevic, B., and Baskarad, M., "Prediction of Internal Ballistic Parameters of Solid Propellant Rocket Motors", *Problem of Mechatronics Armament, Aviation, Safety Engineering*, Vol. 4, pp. 7-26, (2011).
- [6] Hoffmann, K. A., and Chiang, S. T., "*Computational Fluid Dynamics Volume II*", 4th, Edition, Wichita, Kansas, p. 98 (2000).
- [7] Steger, J. L., and Warming, R. F., "Flux Vector Splitting of the in Viscid Gas Dynamic Equations with Application to Finite Difference Methods", *Computational Physics*, Vol. 40, pp. 263-293, (1981).
- [8] Sutton, G.P., and Biblarz, O., "*Rocket Propulsion Elements*", 7th, Edition, John Wiley & Sons, New York, (1992).

- [9] Lenoir, J. M., and Robillard, G., "A Mathematical Method to Predict the Effects of the Erosive Burning in Solid Propellant Rockets", in Proceeding of the 6th Symposium on Combustion, New York, pp. 663-667, (1957).

Nomenclature

u = port axial gas velocity, m/s
 e_t = total specific energy of gas in port, j/kg
 p = gas static pressure, pa
 A_p = port cross-sectional area, m²
 r_b = propellant burning rate, m/s
 P_b = burning perimeter, m
 C_p = gas specific heat, j/kg-K
 C_s = propellant specific heat, j/kg-K
 T_f = gas flame temperature, K
 S_b = burning surface area, m²
 T_s = solid propellant surface temperature, K
 T_p = initial ambient temperature within the solid propellant grain, K
 Pr = Prandtl number ($Pr = \mu C_p/k$)
 k = combustion products thermal conductivity, w/m-K
 R = specific gas constant, j/kg-K
 d_i = initial port diameter, m
 d_f = inner casing diameter, m
 d_t = nozzle throat diameter, m

Greek Symbols

ρ = gas density, kg/m³
 ρ_s = propellant density, kg/m³
 μ = combustion products viscosity, kg/m-s
 γ = Gas specific heat ratio

چکیده

به منظور پیش‌بینی عملکرد موتور موشک سوخت جامد، از یک مدل بالستیک داخلی بر اساس معادلات یک‌بعدی و غیر دائم اویلر استفاده شده است. جریان به صورت گاز ایده‌آل غیرواکنشی در نظر گرفته شده است و خصوصیات ترموفیزیکی جریان، دارای تغییرات زمانی و مکانی هستند. معادلات حاکم بر محفظه احتراق با استفاده از روش تجزیه بردار شار استگر و ورمینگ، به صورت عددی حل شده است. پس از صحت‌گذاری نتایج با داده‌های آزمایشگاهی، اثر تغییر در هندسه گرین و خصوصیات پیشران بر روی خصوصیات عملکردی یک موتور استاندارد با گرین استوانه‌ای درون‌سوز، بررسی شده است. پارامترهای مورد بررسی شامل اثر سوزش فرسایشی، خصوصیات پیشران، نسبت سطح مقطع پورت به گلوگاه و دمای اولیه پیشران است. نتایج نشان داد که خصوصیات پیشران اثر قابل توجهی بر عملکرد موتور موشک دارند و در نظر گرفتن سوزش فرسایشی باعث می‌شود که نتایج تحلیل بالستیک داخلی یک‌بعدی به داده‌های آزمایشگاهی بسیار نزدیک شود.